



## Research Article

**BIOSORPTION OF PHENOL USING MODIFIED BARLEY HUSK: STUDIES ON EQUILIBRIUM ISOTHERM, KINETICS, AND THERMODYNAMICS OF INTERACTIONS****Davoud BALARAK<sup>1</sup>, Kethineni CHANDRIKA<sup>2</sup>, Chinenye Adaobi IGWEGBE\*<sup>3</sup>, Shahin AHMADI<sup>4</sup>, Chinedu Josiah UMEMBAMALU<sup>5</sup>**<sup>1</sup>Department of Environmental Health, Health Promotion Research Center, Zahedan University of Medical Sciences, Zahedan, IRAN; ORCID: 0000-0003-3679-9726<sup>2</sup>Department of Petroleum Engineering, Koneru Lakshmaiah Education Foundation, Vaddeswaram, Guntur, AP, INDIA-52250; ORCID: 0000-0002-1128-2598<sup>3</sup>Department of Chemical Engineering, Nnamdi Azikiwe University, Awka, NIGERIA; ORCID: 0000-0002-5766-7047<sup>4</sup>Department of Environmental Health, School of Public Health, Zabol University of Medical Sciences, Zabol, IRAN; Department of Environmental Health Engineering, School of Public Health, Hamedan University of Medical Sciences, Hamedan, IRAN; ORCID: 0000-0003-2831-2148<sup>5</sup>Department of Chemical Engineering, Nnamdi Azikiwe University, Awka, NIGERIA; ORCID: 0000-0003-2951-1691

Received: 29.05.2020 Revised: 20.07.2020 Accepted: 21.07.2020

**ABSTRACT**

Phenol (PHEN) adsorption using hydrogen chloride (HCl) modified barley husk (MBH) was studied, in which the effects of MBH dose (0.5-4 g/L), initial pH (3-11), contact time (10-180 min), and initial PHEN concentration (10-100 mg/L) were investigated. The adsorbent material was prepared via the chemical activation method. The MBH morphological properties with the surface chemistry characteristics were studied through the Brunauer-Emmett-Teller (BET) surface area, scanning electron microscopy (SEM), Energy Dispersive X-ray Microanalysis (EDX), Fourier-transform infrared (FTIR), and point of zero charge (pHpzc) analyses. The data was examined using the four common models of isotherm (Freundlich, Langmuir, Dubinin-Radushkevich (D-R), and Temkin). The pseudo-first-order, pseudo-second-order, and the intra-particle diffusion models were also used to examine the data. Thermodynamics parameters: free energy change ( $\Delta G^\circ$ ), enthalpy change ( $\Delta H^\circ$ ) and entropy change ( $\Delta S^\circ$ ) were evaluated. MBH was highly efficient due to its high surface area (176.2 m<sup>2</sup>/g). Maximum removal of PHEN (93.95%) occurred at pH 3, MBH dose: 3 g/L, PHEN concentration: 10 mg/L, and contact time: 180 min at a constant temperature of 30 ± 2 °C. The D-R isotherm and pseudo-second-order best represented the isotherm and kinetic data, respectively. The values of  $\Delta G^\circ$  (-0.056, -0.613, -1.431, -2.052, -2.941 and -3.731 kJ/mol),  $\Delta H^\circ$  (23.88 kJ/mol) and  $\Delta S^\circ$  (0.087 kJ/mol K) indicate a feasible, spontaneous and endothermic adsorption process. MBH, a low-cost adsorbent can be used effectively to remove PHEN from PHEN-containing water.

**Keywords:** Phenol, barley husk, adsorption, isotherms, thermodynamics, kinetics.

\* Corresponding Author: e-mail: ca.igwegbe@unizik.edu.ng, tel: +2348036805440

## **1. INTRODUCTION**

Nowadays, the treatment of industrial wastewaters is becoming problematic [1, 2]. Phenols are one of the most common contaminants which can be discovered in water and wastes from oil refineries, chemical plants, textile and pesticide manufacture, explosives, resins, and coke manufacture [3, 4]. PHEN is classified as a hazardous pollutant group since it is highly toxic to organisms and human health even in little concentrations [5]. Since PHENs are dangerous to living organisms at little concentrations, they are considered as significant contaminants [6]. Also, it has been categorized as hazardous contaminants due to its impending harm to human wellbeing [7]. EPA (Environmental Protection Agency) demands to reduce the level of PHEN in wastewaters below 0.5 mg/L owing to its high toxicity [8] and carcinogenic nature [9]; therefore, its reduction in industrial wastewaters is mandatory [10].

Several methods have been useful for the reduction of PHEN levels in water including solvent extraction, chemical oxidation, adsorption, and microbial degradation [11, 12]. It is has been stated that adsorption is the most durable and efficient technique for the removal of PHEN owing to its significant benefits including high efficiency, low operating cost, easy handling, high selectivity, easy regeneration of used adsorbent, and lower production of chemical or biological sludge [13, 14].

Activated carbon is believed as the most extensively exploited adsorbent material to eliminate contaminants from water [15, 16]. Therefore, many inexpensive adsorbents have been evaluated to remove PHENs from effluents [17, 18]. Recently, researchers have used numerous materials as adsorbents such as fungal or bacterial biomass and natural biopolymers, including wheat shells, peat, wood sawdust, fly ash, and dried algal biomass [19, 20].

The barley husk (BH) is one agronomic residue that can be used as low-cost adsorbent material [21]. Recently, the residues of BH are increasingly available due to the increase in the tendency to consume vegetable oils in Iran and the entire world [22, 23]. The residues of BH have been used as an adsorbent in numerous studies and acceptable results have been indicated for the removal of contaminants [24, 25].

In this study, MBH was employed as a biosorbent to eliminate phenol (PHEN) as a target contaminant from an aqueous solution. The aim of this work is to study the effects of influencing parameters of biosorption (MBH dosage, pH, temperature, initial PHEN concentration, and contact time) on the elimination of PHEN using MBH. The isotherm, thermodynamic and kinetics parameters of the removal process were also considered.

## **2. MATERIALS AND METHODS**

### **2.1. Materials**

PHEN was procured from Sigma-Aldrich Co. De-ionized water was used to prepare all solutions for the experiments. The stock solution of PHEN (1000 mg/L) was prepared in 1000 ml volumetric flask at room temperature by suspending an accurate weight of PHEN in deionized water. The working solutions were prepared by diluting the already prepared stock solution to proper concentrations. The general properties and chemical structure of PHEN are shown in Table 1.

### **2.2. Adsorbent preparation**

The barley husks (BH) were collected from farmlands in Tabriz city, Iran. It was sundried, crushed and sieved to particle sizes in the range of 1–2 mm. The biomass was treated with 0.1 M HCl for a period of 5 h, washed with distilled water and dried in the shade. The resultant biomass was used subsequently in the adsorption experiments.

The specific surface area of the MBH before use was determined by Brunauer-Emmett-Teller nitrogen adsorption (BET-N<sub>2</sub>) method based on nitrogen adsorption-desorption isotherms at 77 K. Scanning electron microscopy (SEM) of the MBH was carried out using a scanning microscope (Philips, Eindhoven) equipped with an energy-dispersive X-ray (EDX) (SERON). The FTIR spectra of MBH was recorded in the range of 400–4000 cm<sup>-1</sup> by an FTIR machine (Nicolet 5700 instrument, Thermo Corp., USA) to observe the chemical/functional groups which are accountable for the process of PHEN adsorption.

To ascertain the point of zero charge (pH<sub>ZPC</sub>) of the MBH and BH, 0.1 g of the MBH and 0.1g of BH were added separately to 50 ml of 0.2 mol/L sodium chloride (NaCl). The initial pH of the solution was adjusted to different pHs from 2 to 12 using 0.1 mol/L sodium hydroxide (NaOH) or 0.1 mol/L hydrogen chloride (HCl) solutions. Then the mixtures were shaken in the shaker at 200 rpm and temperature of 30±2°C for 24 h. After equilibrium, the mixtures were filtered and the zeta potentials were measured using a Zetamaster potentiometer.

**Table 1.** Molecular structure and properties of PHEN.

Parameter	Character/ Value
<b>Molecular structure</b>	
<b>CAS number</b>	108-95-2
<b>Molecular formula</b>	C <sub>6</sub> H <sub>5</sub> OH
<b>Molecular weight</b>	94.11 g/mol
<b>Solubility in water</b>	9.3 g PHEN /100 mL H <sub>2</sub> O
<b>Maximum wavelength (λ<sub>max</sub>)</b>	280 nm

### 2.3. Batch adsorption experiments

The most important effective variables on adsorption from the literature include pH, adsorbent dose, contact time, and adsorbate concentrations. Therefore, the effects of initial PHEN concentration (10-100 mg/L), MBH dosage (0.5-4 g/L), contact time (10-180 min) and pH (3-11) were investigated. The batch experiments were carried out in 200 mL Erlenmeyer flasks. In each adsorption experiment, PHEN solution of a certain concentration was added into the flask. The desired pH was set and then a specific dose of MBH adsorbent was added. Then, the mixture was mixed with a shaker at 120 rpm for a certain time. Then, the mixture was centrifuged at 3000 rpm for 10 min. The amount of PHEN adsorbed was calculated according to the following Equation (1) [24]:

$$q_e = \frac{(C_0 - C_e)V}{M} \tag{1}$$

Where q<sub>e</sub> is the amount of PHEN adsorbed (mg/g), C<sub>0</sub> and C<sub>e</sub> are the initial and equilibrium concentrations of liquid phase (mg/L), respectively, V is the volume of the solution (L), and m is the mass of the MBH used. All retention measurements by high-performance liquid chromatography (HPLC) were made with a PerkinElmer Series 200 HPLC apparatus (Shelton, CT, USA) equipped with a column C18 and UV detector set at 280 nm. An injector with 40 μL sample loop was used for all sample injections.

### 3. RESEARCH FINDINGS AND DISCUSSION

#### 3.1. MBH Characterization Results

The definite surface area is linked to the number of active adsorption sites present on an adsorbent material. The adsorption rate increases with the porosity and specific surface area of an adsorbent. The surface area of MBH was revealed as  $176.2 \text{ m}^2/\text{g}$ , which indicates that the MBH has relatively good capability to eliminate PHEN.

Scanning electron microscopy (SEM) images were employed to analyze the surface structure of MBH before and after PHEN adsorption (Figures 1a and 1b). The MBH was found to possess a heterogeneous rough surface structure as well as deep pores which is relatively organized with different sizes and shapes. As seen in Figure 1b, the pores of the MBH were filled with PHEN molecules after adsorption.

The elemental composition analysis of the adsorbent (MBH) performed using the Energy Dispersive Xray Microanalysis (EDX) is shown in Figure 2. Elemental analysis of MBH shows a high yield of carbon (57.57%), oxygen (35.7%), hydrogen (4.40%) and small amounts of calcium (1.2%), potassium (0.75%), sodium (0.77%), phosphorus (0.017%), chlorine (0.24%), and sulphur (0.11%).

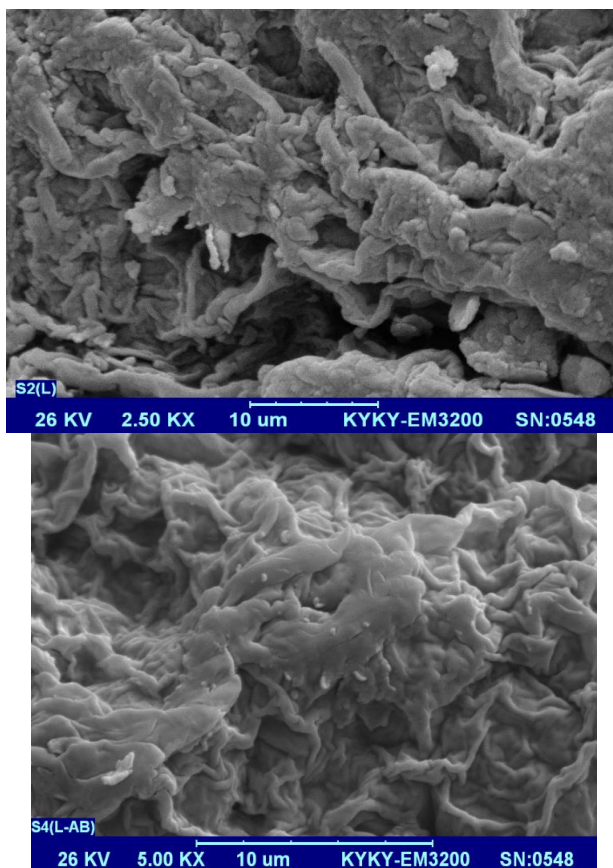


Figure 1. The SEM image of MBH before and after PHEN removal.

In order to understand the interaction between the functional groups existing in MBH and PHEN cations, both MBH before and after use was examined by means of the Fourier transform infrared (FT-IR) spectroscopy. As shown in Figure 3, MBH before and after use showed a similar pattern and the same number of peaks were observed. The peaks at 3410-3430  $\text{cm}^{-1}$  correspond to the O–H stretch due to inter- and intramolecular hydrogen bonding of polymeric compounds for instance alcohols, PHENs, and carboxylic acids, as in pectin, cellulose, and lignin [26]. Thus, showing the presence of free hydroxyl groups on the MPH surface. The peaks at 2928  $\text{cm}^{-1}$  are attributed to the symmetric and asymmetric C–H stretching of aliphatic acids [27]. The peak observed at 1744  $\text{cm}^{-1}$  corresponds to  $-\text{COOH}$ ,  $-\text{COOCH}_3$  stretching of carboxyl groups and may be assigned to carboxylic acids or their esters. The peaks at 1638 and 1413-1418  $\text{cm}^{-1}$  are due to the asymmetric and symmetric stretching vibrations of C=O in ionic carboxylic groups ( $-\text{COO}^-$ ). Aliphatic acid group vibration at 1262  $\text{cm}^{-1}$  may be assigned to C=O and  $-\text{OH}$  stretch of carboxylic acids and PHEN.

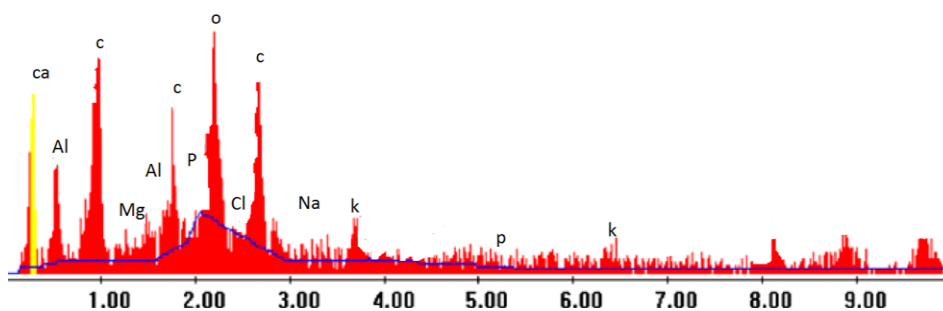


Figure 2. The EDX spectrum of MBH.

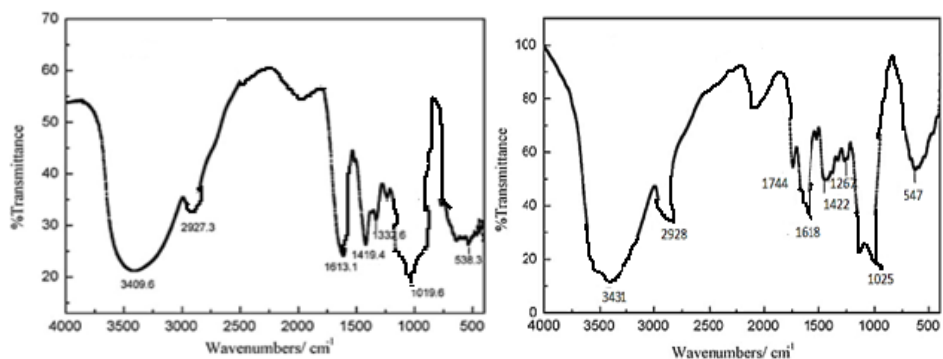


Figure 3. The FT-IR spectra of MBH before and after PHEN removal.

### 3.2. Effect of pH and determination of point of zero charge

The point of zero charge ( $\text{pH}_{\text{ZPC}}$ ) is a concept relating to the phenomenon of adsorption.  $\text{pH}_{\text{ZPC}}$  can be defined as the pH value at which a solid submerged in an electrolyte exhibits zero net electrical charge on the surface. As observed in Figure 4, the  $\text{pH}_{\text{ZPC}}$  values for BH and MBH are approximately 5.9 and 5.1, respectively. This revealed that the activation by HCl increases the acidic properties of MBH as a result of the hydrogen bonding present. The surface charge becomes positive at  $\text{pH} < \text{pH}_{\text{ZPC}}$  and negative at  $\text{pH} > \text{pH}_{\text{ZPC}}$  [28].

PHEN removal on MBH decreased significantly by increasing the solution pH from 3 to 11 (Figure 5). One of the most important factors affecting the biosorption of PHEN on MBH was the acidity of the solution since the pH of the solution impacts not only the surface charge of the biosorbent and the dissociation of functional groups of the active sites on the biosorbent surface, but as well as the aqueous chemistry of the PHEN [29]. At this pH solution =  $pH_{ZPC}$ , the net surface charge density of MBH is near to zero, and this enhances the  $\pi$ - $\pi$  dispersion interaction. Consequently, when the solution  $pH > pH_{ZPC}$ , the surface charge density of MBH is negative and PHEN is deprotonated. As a result, the repulsive electrostatic interaction is intensified [30]. This is the main mechanism that contributed to the weak adsorption efficiency onto MBH at  $pH > pH_{ZPC}$ . These results were consistent with the previous study on the adsorptive removal of PHEN onto Azolla [31]. Kadhim et al. [32] examined the effect of initial pH on the removal of PHEN from aqueous solution onto rice husk. As pH increased from 3 to 11, the adsorption capacity decreased from 15.2 to 5 mg/g at 100 mg/L concentration; maximum uptake was observed at pH 3.0.

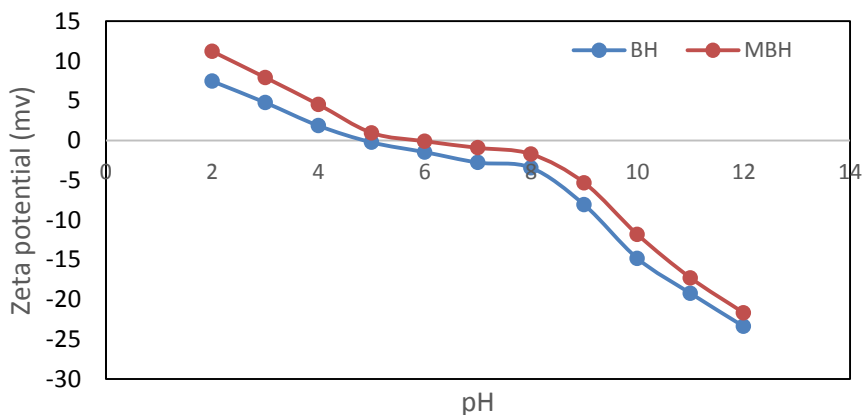


Figure 4. Determination of the point of zero charges of BH and MBH.

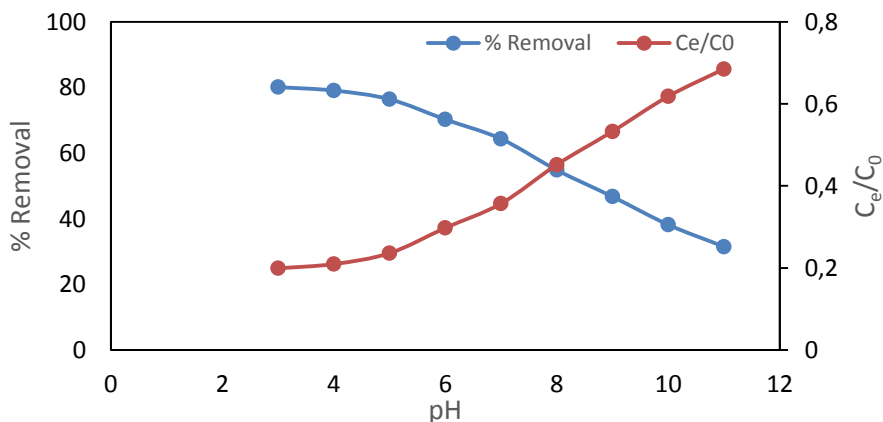
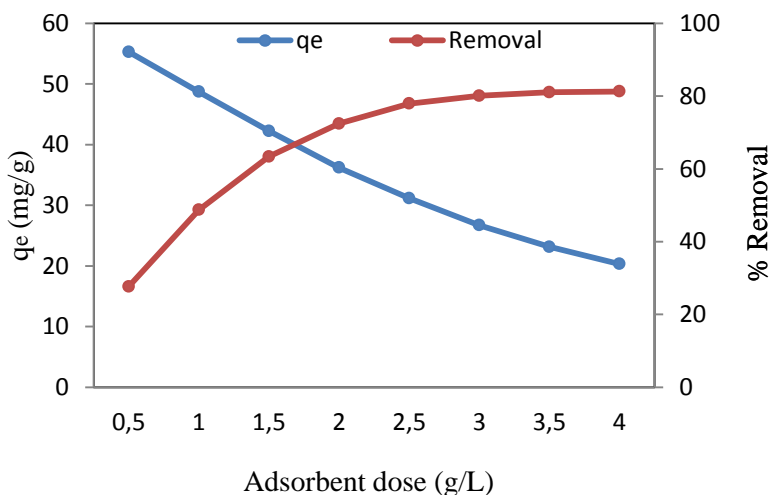


Figure 5. Influence of pH on PHEN removal (contact time = 90 min, dosage = 3 g/L, PHEN concentration  $C_0$ : 100 mg/L, temperature =  $30 \pm 2$  °C).

### 3.3. Effect of adsorbent dosage

The effect of MBH dose on PHEN removal was studied to determine the optimum MBH dosage. As shown in Figure 6, the efficiency of PHEN removal improved with increasing the MBH dosage from 0.5 to 4 g/L; the adsorption capacity decreased with increasing dosage. Lower biosorption capacity at a higher dosage of biosorbent is probably as a result of the decrease of the surface area of the biosorbent by the overlapping or aggregation during the process of sorption [33]. However, a higher dosage of MBH led to the greater availability of active sites for PHEN, resulting in higher PHEN removal [34]. Similarly, Diyanati et al. [31] investigated the influence of dose on the PHEN removal from aqueous solution; the removal efficiency increased from 27.65% to 81.27%, while the  $q_e$  decreased from 55.3 to 20.31 mg/g by increasing the biosorbent dose from 0.5 to 4 g/L.



**Figure 6.** Influence of MBH dose on PHEN removal (contact time = 90 min, pH = 3, PHEN concentration  $C_0 = 100$  mg/L, temperature =  $30 \pm 2$  °C).

### 3.4. Effect of contact time and initial PHEN concentration

Figure 7 indicates that PHEN removal improved as the contact time was increased from 10 to 180 min. Equilibrium was met at 120 min. Therefore, the optimum contact time for PHEN removal on MBH is considered to be 120 min. At the initial times, PHEN removal was rapid. The gradient of adsorption declined with time which may be due to declining concentration of PHEN and decreasing active adsorption sites on the adsorbent surface area [27]. In the early stages of adsorption, there were lots of empty spaces and they were occupied with time by PHEN molecules [35]. Similarly, Dursun et al. [36] investigated the effect of agitation time on the removal of PHEN from aqueous solution on carbonized beet pulp. The results showed that the adsorption capacity (mg/g) increased with increasing time. The equilibrium was established after 120 min of contact time.

PHEN adsorption on MBH decreased with increasing PHEN concentration from 10 to 100 mg/L. The results are shown in Figure 7. As indicated, 93.95% removal was obtained at 10 mg/L concentration; removal of PHEN decreased with increasing initial concentration and reached 72% at the concentration of 200 mg/L. This probably occurred due to the increasing surface charge on the adsorbent; the adsorption sites of the top surfaces of the adsorbent were saturated and the

removal efficiency decreased [37]. Dakhil [38] investigated the effect of concentration on the removal of PHEN from aqueous solution. The removal percent decreased from 90% to 80% with increasing PHEN concentration from 10 to 50 mg/L.

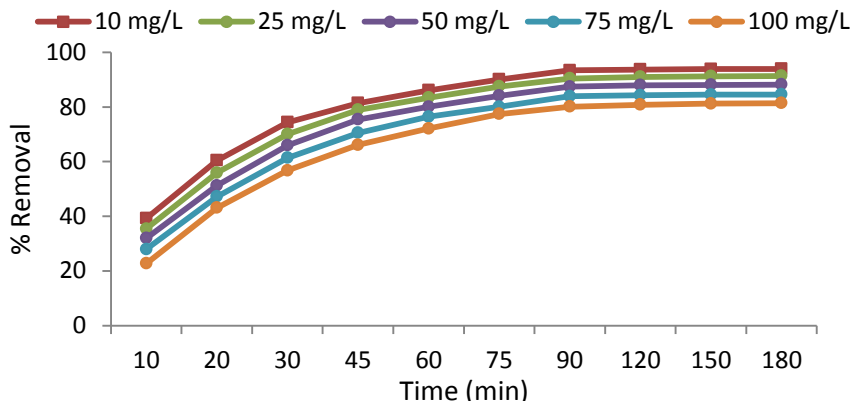


**Figure 7.** Effect of contact time and initial PHEN concentration (pH = 3, dose = 3 g/L, temperature = 30 ± 2 °C)

### 3.5. Adsorption isotherms

The equilibrium data is important in the design of adsorption systems [39]. Although several isotherm equations are available, four important isotherms (Freundlich, Langmuir, Temkin, and Dubinin-Radushkevich) were selected for this study. The Langmuir isotherm is expressed as Equation (2) [40]:

$$\frac{C_e}{q_e} = \frac{1}{q_m K_L} + \frac{C_e}{q_m} \quad (2)$$

Where  $q_e$  (mg/g) and  $C_e$  (mg/L) are the equilibrium concentration of PHEN in the solid and liquid phases, respectively;  $q_m$  (mg/g) is the maximum theoretical biosorption capacity;  $K_L$  (L/mg) is a measure of biosorption energy, showing the affinity between biosorbent and sorbate. A straight-line plot of  $C_e/q_e$  versus  $C_e$  gives an intercept of  $1/q_m \cdot K_L$  and slope of  $1/q_m$ .

The essential feature of the Langmuir isotherm can be expressed in terms of a dimensionless constant called separation factor ( $R_L$ ), also known as equilibrium parameter which is defined by Equation (3) [39, 41]:

$$R_L = \frac{1}{1 + C_0 K_L} \quad (3)$$

Where  $C_0$  (mg/L) is the initial PHEN concentration. The value of  $R_L$  specifies the shape of the isotherms to be either unfavorable ( $R_L > 1$ ), linear ( $R_L = 1$ ), favorable ( $0 < R_L < 1$ ) or irreversible ( $R_L = 0$ ).

The Freundlich isotherm model can be expressed logarithmically as in Equation (4) [42]:

$$\text{Log } q_e = \frac{1}{n} \text{log } C_e + \text{log } K_F \quad (4)$$

$K_F$  [(mg/g)/(mg/l)<sup>1/n</sup>] is the Freundlich constant related to the sorption capacity of the adsorbent and  $1/n$  is the Freundlich constant associated to the energy heterogeneity of the system and the size of the adsorbed molecule. The values of  $K_F$  and  $n$  can be estimated from the linear plot of  $\text{Log } q_e$  versus  $\text{Log } C_e$ .

Temkin isotherm proposes an equal distribution of binding energies over the number of the exchanging sites on the surface. The linear form of Temkin isotherm can be written as [43]:

$$q_e = B \ln A + B \ln C_e \tag{5}$$

Where  $B=RT/b$ ,  $T$  is the absolute solution temperature and  $R$  is the universal gas constant (8.314 J/mol.K).  $A$  is the equilibrium binding constant and  $B$  is related to the heat of sorption. The values of  $B$  and  $A$  can be determined from the plot of  $q_e$  versus  $\ln C_e$ .

The Dubinin-Radushkevich (D-R) model can be expressed independently of solution temperature using the adsorption potential ( $\epsilon$ ) (Equation 6) [44]:

$$\epsilon = RT \ln \left(1 + \frac{1}{C_e}\right) \tag{6}$$

The D-R isotherm assumes a Gaussian-type distribution for the characteristic curve and the model can be described by Equation (7) [45, 46]:

$$\ln q_e = \ln q_m - \beta \epsilon^2 \tag{7}$$

Where  $q_m$  is the D-R constant (mol/g) and  $B$  gives the mean sorption free energy,  $E$  (kJ/mol) per molecule of sorbate at the moment of its transfer to the solid surface from the solution and can be computed using Equation (8) [45]:

$$E = (-2K)^{-1/2} \tag{8}$$

Plotting  $\ln q_e$  versus  $\epsilon^2$ , using Eq. (8), results in a straight-line of slope,  $\beta$ , and intercept,  $\ln(q_m)$ .

Figures 8a-d show the Freundlich, Langmuir, Temkin, and Dubinin-Radushkevich plots, with the calculated parameters are summarized in Table 2. As seen in Table 2, D-R isotherm favors the PHEN uptake by MBH ( $R^2=0.971$ ) than the other models. The values of  $R^2$  reveal that the experimental data fitted into the D-R isotherm model.

It is reported that when the value of  $E$  is below 8 kJ/mol, the process of adsorption can be considered as physisorption [47]. In contrast, if the value of  $E$  is located within the range of 8-16 kJ/mol, it is a chemisorption process. From Table 2, it can be seen that the obtained value of mean free energy,  $E$ , is 0.267 kJ/mol. Based on these, it can thus be concluded that the effect of physical adsorption will play a dominating role in the process of PHEN adsorption on the MBH.

Furthermore, Freundlich isotherm constant can be used to explore the favorability of the process of adsorption. The process is said to be favorable when the value of  $n$  satisfies the condition  $1 < n < 10$ , otherwise it is unfavorable. The  $1/n$  value of 0.667 (Table 2) for the adsorption of PHEN on MBH is found to be within 0 and 1 indicating desirable adsorption process and heterogeneity of the process [48].

**Table 2.** Adsorption isotherm constants for the adsorption of PHEN onto MBH.

Langmuir model				Freundlich model			Temkin model			D-R model		
$q_m$	$K_L$	$R_L$	$R^2$	$1/n$	$K_F$	$R^2$	$A$	$B$	$R^2$	$q_m$	$E$	$R^2$
111.1	0.015	0.393	0.821	0.667	3.51	0.895	6.81	24.15	0.963	56.75	0.267	0.971

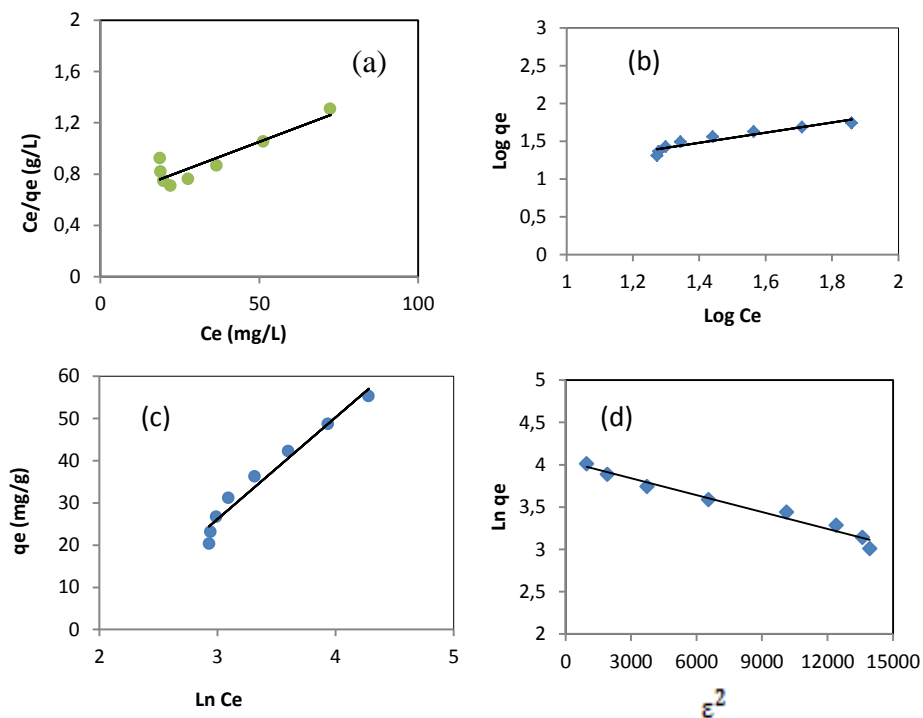


**Figure 8.** Linear fitting plots of (a) Langmuir, (b) Freundlich, (c) Temkin and (d) D-R isotherm models.

### 3.6. Adsorption kinetics

In order to examine the mechanism in control of the adsorption process, pseudo-second-order, pseudo-first-order, and intraparticle diffusion kinetic equations were used to examine the kinetic data. The pseudo-first-order rate equation is expressed as Equation (9) [49, 50]:

$$\text{Log } (q_e - q_t) = \text{Log } q_e - \frac{K_1 t}{2.3} \quad (9)$$

Where  $q_e$  and  $q_t$  are the amounts of PHEN adsorbed (mg/g) at equilibrium and at time  $t$  (min), respectively;  $K_1$  is the rate constant of adsorption ( $\text{min}^{-1}$ ).  $K_1$  values were estimated from  $\text{Log } (q_e - q_t)$  versus  $t$  plots at various concentrations.

The pseudo-second-order model equation is expressed as Equation (10) [51, 52]:

$$\frac{t}{q} = \frac{1}{K_2 q_e^2} + \frac{t}{q_e} \quad (10)$$

Where  $K_2$  is the rate constant of pseudo-second-order ( $\text{g mg}^{-1} \text{min}^{-1}$ );  $q$  and  $q_e$  are the amounts of solute adsorbed at any time and at equilibrium (mg/g), respectively.

The two models were able to define the adsorption data. The agreement between the calculated data and experimental values is expressed by the correlation coefficient ( $R^2$ ). The results are presented in Table 3 and Figures 9-10. Kinetic data of PHEN onto MBH fit the pseudo-second-order model ( $R^2 > 0.992$ ) than the pseudo-first-order model ( $R^2 > 0.971$ ) proposing a chemisorption process [47].

The intraparticle diffusion rate equation is expressed as Equation (11) [53]:

$$q_t = K_i t^{1/2} + C \tag{11}$$

Where C is the intercept and  $K_i$  is the intraparticle diffusion rate constant ( $\text{mg/gmin}^{1/2}$ ), which can be evaluated from the slope of the linear plot of  $q_t$  versus  $t^{1/2}$ .

Intra-particle diffusion is the rate-limiting step when the plot passes through the origin ( $C=0$ ). If the value of C is higher than zero, the difference in the rate of mass transfer during the early and final stages occurred. It is observed from Figure 11 that the plot did not pass through the origin (the value of  $C>0$ ), hence the PHEN adsorption mechanism is probably a combination of boundary layer and pore diffusion. Both contributed to the rate-determining step. Therefore, the adsorption of PHEN ions on the MBH surface is complex, involving more than one mechanism as shown in Figure 11.

**Table 3.** Calculated parameters of kinetics for PHEN adsorption on MBH.

$C_o$ (mg/L)	$q_e$ (mg/g)	Pseudo-first-order			Pseudo-second-order			Intraparticle diffusion		
		$K_1$ ( $\text{min}^{-1}$ )	$q_e$ (mg/g)	$R^2$	$K_2$ ( $\text{g mg}^{-1}\text{min}^{-1}$ )	$q_e$ (mg/g)	$R^2$	$K_i$ ( $\text{mg/gmin}^{1/2}$ )	C	$R^2$
10	3.131	0.046	3.11	0.971	0.025	3.401	0.997	0.155	1.406	0.75
25	7.614	0.043	7.66	0.988	0.009	8.403	0.998	0.403	30.14	0.757
50	14.691	0.039	17.45	0.983	0.004	16.39	0.996	0.824	5.556	0.764
75	21.14	0.042	25.75	0.976	0.002	23.80	0.995	1.256	7.178	0.775
100	27.12	0.049	32.19	0.992	0.002	31.25	0.992	1.735	7.774	0.782

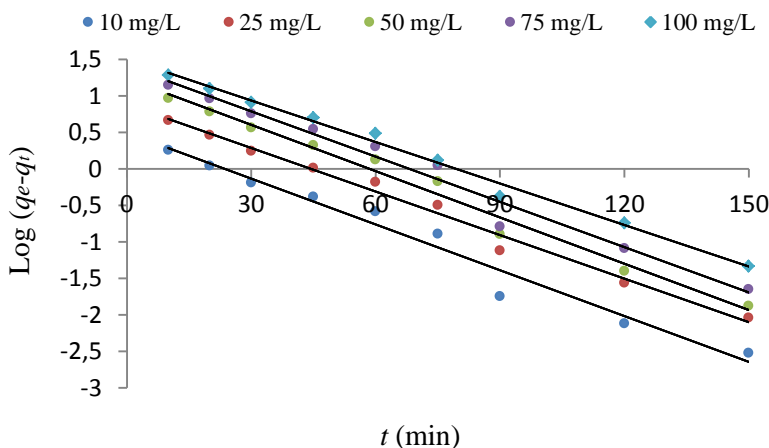


**Figure 9.** Pseudo-first-order kinetic model for PHEN adsorption on MBH.

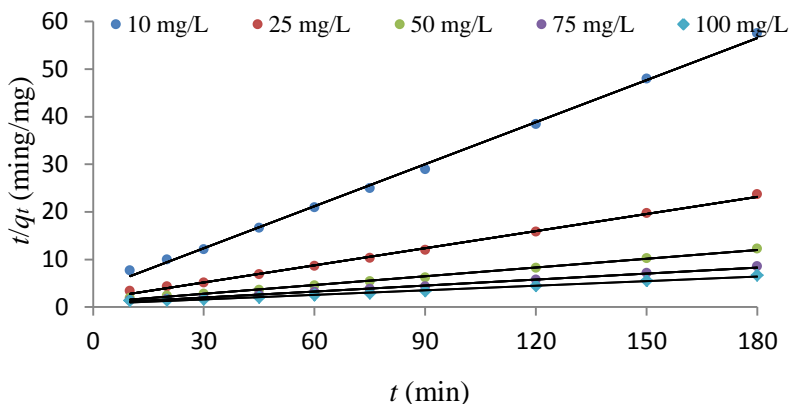


**Figure 10.** Pseudo-second-order kinetic model for PHEN adsorption on MBH.

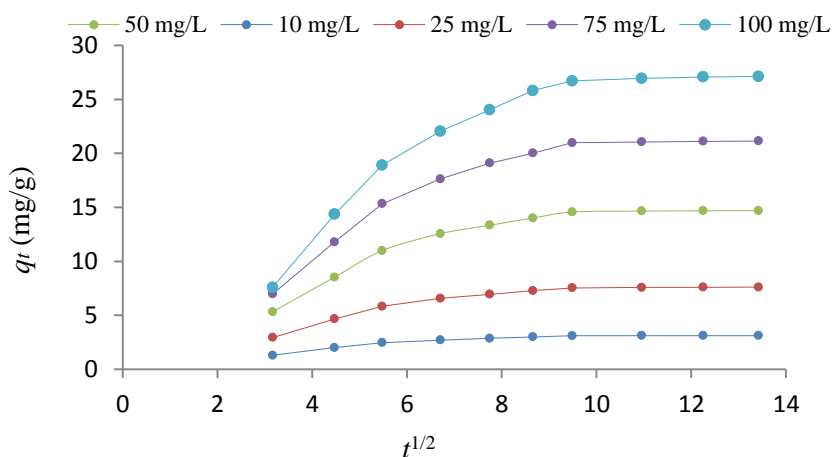


**Figure 11.** Intraparticle diffusion plot of PHEN adsorption at various concentrations.

### 3.7. Thermodynamic analysis

To evaluate the effect of temperature on the PHEN adsorption on MBH, the free energy change ( $\Delta G^\circ$ ), enthalpy change ( $\Delta H^\circ$ ), and entropy change ( $\Delta S^\circ$ ) were determined using the following equations [54-56]:

$$\ln K_L = -\frac{\Delta H^\circ}{RT} + \frac{\Delta S^\circ}{R} \tag{12}$$

$$\Delta G^\circ = \Delta H^\circ - T\Delta S^\circ \tag{13}$$

Where  $K_L$  is the Langmuir equilibrium constant (L/mol); R is the gas constant (8.314 J/mol K); T is the solution temperature (K).

Considering the connection between  $\Delta G^\circ$  and  $K_L$ ,  $\Delta H^\circ$  and  $\Delta S^\circ$  were evaluated from the slope and intercept of the Van't Hoff plots of  $\ln(K_L)$  versus  $1/T$  (Figure 12). Table 4 presents the parameters of thermodynamic at different temperatures (273, 283, 293, 303, 313 and 323 K). The

negative values of  $\Delta G^\circ$  confirm the feasibility and spontaneity of the process [57].  $\Delta G^\circ$  values were found to decrease from  $-0.056$  to  $-3.73$  kJ/mol. The decrease in the  $\Delta G^\circ$  negativity value with increasing temperature indicates that the PHEN removal on MBH becomes more favorable at greater temperatures. The  $\Delta H^\circ$  and  $\Delta S^\circ$  values calculated from the plot of  $\ln(K_L)$  versus  $1/T$  are given as  $23.88$  kJ/mol and  $0.087$  kJ/mol.K, respectively. Zheng et al. [58] suggested that the  $\Delta H^\circ$  of physisorption is smaller than  $40$  kJ/mol. The value of  $\Delta H^\circ$  ( $23.88$  kJ/mol) suggests that the process is a physisorption process. The  $\Delta H^\circ$  value was positive, showing that the reaction was endothermic. The positive value of  $\Delta S^\circ$  reflects the affinity of the MBH for PHEN; this also suggests some structural changes in PHEN and MBH [57].

**Table 4.** Calculated parameters of thermodynamics for PHEN adsorption on MBH.

Temperature (°K)	$\Delta G^\circ$ (kJ/mol)	$\Delta H^\circ$ (kJ/mol)	$\Delta S^\circ$ (kJ/mol K)
273	-0.056		
283	-0.613		
293	-1.431	23.88	0.087
303	-2.052		
313	-2.941		
323	-3.731		

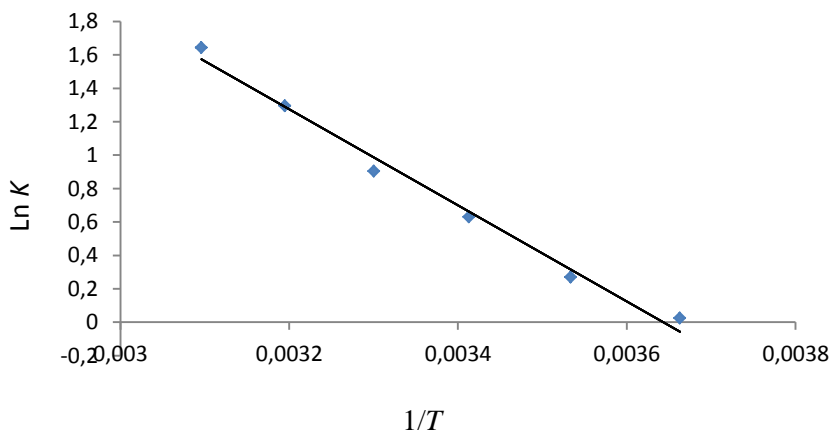


**Figure 12.** Van't Hoff plot for PHEN removal on MBH.

### 3.8. Comparison of MBH with other adsorbents for PHEN removal

See Table 3 by Igwegbe et al. [57] which shows the comparison of gypsum with other materials for PHEN reduction. For this study, maximum PHEN removal of 93.95% was obtained using MBH at pH 3, MBH dose: 3 g/L, PHEN concentration: 10 mg/L, and contact time: 180 min at a constant temperature of  $30 \pm 2$  °C. This indicates that MBH can also be considered as a good biosorbent for the removal of phenol from water.

## 4. CONCLUSIONS

The modified barley husk (MBH) was used as a biosorbent to remove phenol (PHEN) from its solution. PHEN removal was dependent on the MBH dosage, pH, initial PHEN concentration, contact time, and temperature. The results showed that PHEN removal increased with increasing solution temperature. Various kinetic models were tested to analyze the mechanism of the process

of adsorption; the pseudo-second-order model agreed with the dynamic behavior of PHEN removal onto MBH. The adsorption data fitted well to the D-R model. The negative values of  $\Delta G^\circ$  indicated the spontaneity and favorability of the PHEN adsorption on MBH. The positive values of  $\Delta H^\circ$  and  $\Delta S^\circ$  showed the endothermic nature and irreversibility of the process, respectively. This research has revealed that MBH can be efficiently used to remove PHEN ions from aqueous solutions.

### Acknowledgments

The authors are grateful to the deputy of research and technology of Zahedan University of Medical Sciences.

### REFERENCES

- [1] Santos V.L., Monteiro A., Braga D., Santoro, M., (2009) Phenol degradation by *Aureobasidium* pollutants FE13 isolated from industrial effluents, *Journal of Hazardous Materials* 161:1413-1420.
- [2] Zazouli M.A., Mahdavi Y., Bazrafshan E., (2014) Photodegradation potential of bisphenol from aqueous solution by *Azolla Filiculoides*, *Journal of Environmental Health Science & Engineering* 12(66).
- [3] Senturk H.B., Ozdes D., Gundogdu A., Duran C., Soylak, M., (2009) Removal of phenol from aqueous solutions by adsorption onto organomodified Tirebolu bentonite, *Journal of Hazardous Materials* 172:353-362.
- [4] Kumar N.S., Subbaiah M.V., Reddy A.S., Krishnaiah A., (2009) Biosorption of phenolic compounds from aqueous solutions onto chitosan–*abrus precatorius* blended beads, *Journal of Chemical Technology & Biotechnology* 84:972-981.
- [5] Balarak D., (2016) Kinetics, isotherm and thermodynamics studies on bisphenol adsorption using barley husk, *International Journal of ChemTech Research* 9(5):681-90.
- [6] Zhou Y., Lu P., Lu J., (2012) Application of natural biosorbent and modified peat for bisphenol a removal from aqueous solutions, *Carbohydrate Polymers* 88(2):502-508.
- [7] Kamble S.P., Mangrulkar P.A., Bansiwai A.K., Rayalu S.S., (2008) Adsorption of phenol and o-chlorophenol on surface altered fly ash based molecular sieves, *Chemical Engineering Journal* 138:73-83.
- [8] Xiao M., Zhou J., Tan Y., Zhang A., Xia Y., Ji L., (2006) Treatment of highly-concentrated phenol wastewater with an extractive membrane reactor using silicone rubber, *Desalination* 195:281-93.
- [9] Ahmadi S., Igwegbe C.A., (2018) Adsorptive removal of phenol and aniline by modified bentonite: adsorption isotherm and kinetics study, *Applied Water Science* 8:170.
- [10] Park J.S., Brown M.T., Hana T., (2012) Phenol toxicity to the aquatic macrophyte *Lemna paucicostata*, *Aquatic Toxicology* 106-107:182–188.
- [11] Rubin E., Rodríguez P., Herrero R., (2008) Biosorption of phenolic compounds by the brown alga *Sargassum muticum*, *Journal of Chemical Technology & Biotechnology* 81:1093-1099.
- [12] Singh S, Melo J.S., Eapen S., D'Souza S.F., (2013) Phenol removal using *Brassica juncea* hairy roots: Role of inherent peroxidase and  $H_2O_2$ , *Journal of Biotechnology* 123:43-49.
- [13] Balarak D., Mostafapour F.K., Le S.M, Jeon C., (2019) Adsorption of Bisphenol a using dried rice husk: equilibrium, kinetic and thermodynamic studies, *Applied Chemical Engineering* 30(3):316-323.
- [14] Diyanati R.A., Yazdani J., Balarak D., (2013) Effect of sorbitol on phenol removal rate by *lemna minor*, *Journal of Mazandaran University of Medical Science* 22(87):58-64.

- [15] Kermani M., Pourmoghaddas H., Bina B., Khazaei Z., (2006) Removal of phenol from aqueous solutions by rice husk ash and activated carbon, *Pakistan Journal of Biological Sciences* 9:1905-1910.
- [16] Nadavala S.K., Swayampakula K., Boddu V.M., Abburi K., (2009) Biosorption of phenol and o-chlorophenol from aqueous solutions on to chitosan-calcium alginate blended beads, *Journal of Hazardous Materials* 162:482-489.
- [17] Khan M.Z., Kanti P., Sabira S.M., (2011) Bioremediation of 2-chlorophenol containing wastewater by aerobic granules-kinetics and toxicity, *Journal of Hazardous Materials* 19:222-8.
- [18] Shen D., Fan J., Zhou W., Gao B., Yue Q., Kang Q., (2009) Adsorption kinetics and isotherm of anionic dyes onto organo-bentonite from single and multisolute systems, *Journal of Hazardous Materials* 172:99-107.
- [19] Busca G., Berardinelli S., Resini C., Arrighi L., (2008) Technologies for the removal of phenol from fluid streams: A short review of recent developments, *Journal of Hazardous Materials* 160:265-288.
- [20] Diyanati R.A., Yousefi Z., Cherati J.Y., (2013) Adsorption of phenol by modified azolla from aqueous solution, *Journal of Mazandaran University of Medical Science* 22(2):13-21.
- [21] Din M., Bhatti H.N., Yasir M., Ashraf A., (2015) Direct dye biosorption by immobilized barley husk, *Desalination Water Treatment* 54; 45-53.
- [22] Maleki A., Mahvi A.H., Zazouli M.A., Izanloo H., Barat A.H., Aqueous cadmium removal by adsorption on barley hull and barley hull ash, *Asian Journal of Chemistry* 23(3):1373-1376.
- [23] Haq I., Bhatti H.N., Asgher M., (2011) Removal of solar red BA textile dye from aqueous solution by low cost MBH: Equilibrium, kinetic and thermodynamic study, *Canadian Journal of Chemical Engineering* 89(3):593-600.
- [24] Robinson T., Chandran B., Nigam P., (2002) Removal of dyes from an artificial textile dye effluent by two agricultural waste residues, corncob and barley husk, *Environment International* 28(1-2):29-33.
- [25] Robinson T., Chandran B., Nigam P., (2002) Effect of pretreatments of three waste residues, wheat straw, corncobs and barley husks on dye adsorption, *Bioresource Technology* 85(2):119-124.
- [26] Varghese S., Vinod V.P., (2004) Kinetic and equilibrium characterization of phenols adsorption onto a novel activated carbon in water treatment, *Indian Journal of Chemical Technology* 11:825-833.
- [27] Uddin M.T., Islam M.S., Adedin M.Z., (2007) Adsorption of phenol from aqueous solution by water hyacinth ash, *Journal of Engineering and Applied Sciences* 2(2):94-99.
- [28] Mahvi A.H., Maleki A., Eslami, A., (2004) Potential of rice husk and rice husk ash for phenol removal in aqueous systems, *American Journal of Applied Sciences* 14:321-326.
- [29] Kennedy L.J., Vijaya J.J., Kayalvizhi K., Sekaran G., (2007) Adsorption of phenol from aqueous solutions using mesoporous carbon prepared by two-stage process, *Chemical Engineering Journal* 132:279-287.
- [30] Kilic M., Apaydin-Varol E., Putin A.E., (2011) Adsorptive removal of phenol from aqueous solutions on activated carbon prepared from tobacco residues: Equilibrium, kinetics and thermodynamics, *Journal of Hazardous Materials* 189:397-403.
- [31] Diyanati R.A., Yousefi Z., Cherati J.Y., (2014) The ability of azolla and lemna minor biomass for adsorption of phenol from aqueous solutions, *Journal of Mazandaran University Medical Science* 23:17-23.
- [32] Kadhim F.A.S., Al-Seroury F.A., (2012) Characterization the removal of phenol from aqueous solution in fluidized bed column by rice husk adsorbent, *Research Journal of Recent Sciences* 1:145-151.

- [33] Moyo M., Mutare E., Chigondo F., Nyamunda B.C., (2012) Removal of phenol from aqueous solution by adsorption on yeast, *Saccharomyces cerevisiae*, *International Journal of Recent Research and Applied Studies* 11(3):486-495.
- [34] Caetano M., Valderrama C., Farran A., Cortina J.L., (2009) Phenol removal from aqueous solution by adsorption and ion exchange mechanisms onto polymeric resins, *Journal of Colloidal Interface Science* 338: 402-409.
- [35] Păcurariu C., Mihoc G., Popa A., Muntean S.G., Ianoş R., (2013) Adsorption of phenol and p-chlorophenol from aqueous solutions on poly functionalized materials, *Chemical Engineering Journal* 222: 218-227.
- [36] Dursun G.U., Cicek H., Dursun A.Y., (2005) Adsorption of phenol from aqueous solution by using carbonised beet pulp”, *Journal of Hazardous Materials* 125:175-182.
- [37] Tagreed L.A., (2011) Removal of phenol from aqueous solution by agriculture waste, *Journal of Engineering & Technology* 28(19):28-35.
- [38] Dakhil. I.H., (2013) Removal of phenol from industrial wastewater using sawdust, *Research Inventy: International Journal of Engineering and Science* 3(1):25-31.
- [39] Igwegbe C.A., Mohmmadi L., Ahmadi S., Rahdar A., Khadkhodaiy D., Dehghani R., Rahdar S., (2019) Modeling of adsorption of Methylene blue dye on Ho-CaWO<sub>4</sub> nanoparticles using Response surface methodology (RSM) and Artificial neural network (ANN) techniques, *MethodsX* 6:1779-1797.
- [40] Yoshida S., Iwamura S., Ogino I., Mukai S.R., (2016) Adsorption of phenol in flow systems by a monolithic carbon cryogel with a micro honeycomb structure, *Adsorption* 22:1051–1058.
- [41] Su J., Lin H.F., Wang Q.P., (2011) Adsorption of phenol from aqueous solutions by organo-montmorillonite, *Desalination* 269:163–169.
- [42] Kuleyin A., (2007) Removal of phenol and 4-chlorophenol by surfactant-modified natural zeolite, *Journal of Hazardous Materials* 144:307–15.
- [43] Baker H.M., Ghanem R., (2009) Evaluation of treated natural zeolite for the removal of o-chlorophenol from aqueous solution, *Desalination*, 249:1265–72.
- [44] Wang S.L., Tzou Y.M., Lua Y.H., Sheng G., (2007) Removal of 3-chlorophenol from water using rice-straw-based carbon, *Journal of Hazardous Materials* 147:313–318.
- [45] Balarak D., Joghataei A., (2016) Biosorption of phenol using dried rice husk biomass: Kinetic and equilibrium studies, *Der Pharma Chemica* 8(6):96-103.
- [46] Ghadim E.E., Manouchehri F., Soleimani G., Hosseini H., Kimiagar S., Nafisi S., (2013) Adsorption properties of tetracycline onto graphene oxide: equilibrium, kinetic and thermodynamic studies, *PLoS ONE* 8(11):e79254.
- [47] Igwegbe C.A., Onyechi P.C., Onukwuli O.D., (2015) Kinetic, isotherm and thermodynamic modelling on the adsorptive removal of malachite green on *Dacryodes edulis* seeds, *Journal of Scientific and Engineering Research* 2:23-39.
- [48] Igwegbe C.A., Rahdar S., Rahdar A., Mahvi A.H., Ahmadi S., Banach A.M., (2019) Removal of fluoride from aqueous solution by nickel oxide nanoparticles: equilibrium and kinetic studies, *Fluoride* 52(4):569-579.
- [49] Ahmadi S., Igwegbe C.A., Rahdar S., Asadi Z., (2019) The survey of application of the linear and nonlinear kinetic models for the adsorption of nickel (II) by modified multi-walled carbon nanotubes, *Applied Water Sciences* 9:98.
- [50] Nayak P.S., Singh B.K., (2007) Removal of phenol from aqueous solutions by sorption on low cost clay, *Desalination* 207:71–79.
- [51] Mukherjee S., Kumar S.A., Misra K., Fan M., (2007) Removal of phenols from water environment by activated carbon, bagasse ash and wood charcoal, *Chemical Engineering Journal* 129:133–142.

- [52] Ahmadi S., Rahdar A., Rahdar S. , Igwegbe C.A., (2019) Removal of Remazol Black B from aqueous solution using P- $\gamma$ -Fe<sub>2</sub>O<sub>3</sub> nanoparticles: synthesis, physical characterization, isotherm, kinetic and thermodynamic studies, *Desalination and Water Treatment* 152:401–410.
- [53] Radhika M., Palanivelu K., (2006) Adsorptive removal of chlorophenols from aqueous solution by low cost adsorbent-kinetics and isotherm analysis, *Journal of Hazardous Materials* B138:116–124.
- [54] Igwegbe C.A., Banach A.M., Ahmadi S., (2018) Adsorption of Reactive Blue 19 from aqueous environment on magnesium oxide nanoparticles: kinetic, isotherm and thermodynamic studies, *Pharmaceutical and Chemical Journal* 5:111-121.
- [55] Soni H., Padmaja P., (2014) Palm shell based activated carbon for removal of bisphenol A: equilibrium, kinetic and thermodynamic study, *Journal of Porous Materials* 21:275-284.
- [56] Yu J., Zhao X., Yang, H., et al., (2014) Aqueous adsorption and removal of organic contaminants by carbon nanotubes, *Science of the Total Environment* 241-251.
- [57] Igwegbe C.A., Al-Rawajfeh A.E., Al-Itawi H.I., Al-Qazaqi S., Hashish E.A., Al-Qatatsheh M., Sharadqah S., Sillanpaa M., (2019) Utilization of calcined gypsum in water and wastewater treatment: removal of phenol, *Journal of Ecological Engineering* 20(7):1–10.
- [58] Zheng S., Sun Z., Park Y., et al., (2013) Removal of bisphenol A from wastewater by Camontmorillonite modified with selected surfactants, *Chemical Engineering Journal* 234:416-422.